Evaluation of Rocket Plume Signature Uncertainties

H.F. Nelson*
University of Missouri—Rolla, Rolla, Missouri

A method is developed with which to evaluate the uncertainty in predictions of the infrared signature of metalized fuel, solid-propellant rocket plumes. The method consists of 1) identifying parameters that represent the major sources of uncertainty, 2) evaluating the infrared signature as each parameter is varied about its nominal value, 3) determining the uncertainty interval of each parameter and 4) root sum squaring the uncertainties to obtain the uncertainty factor for the infrared signature. Uncertainties in the index of refraction, particle size, temperature and number density, gas mole fraction temperature, plume pressure and radius, and Al_2O_3 melting temperature, are considered. These uncertainties are combined to yield an overall uncertainty in the plume infrared emission and a relative ranking of the importance of each uncertainty parameter. Numerical results are generated using the standardized infrared radiation model (SIRRM) code for a solid-propellant tactical rocket plume. The most important parameters in the tactical rocket signature uncertainty are 1) Al_2O_3 particle temperature, the real part of the refractive index and plume radius at 90 deg aspect angle and 2) the real part of the Al_2O_3 particle refractive index, the Al_2O_3 particle temperature and size, and plume size at a nose-on aspect angle.

Nomenclature

f_i = parameter f_i/(nominal value of parameter f_i)
I = radiant intensity, W/cm^2
$\bar{I}$ = intensity/(nominal value of radiant intensity)
k = imaginary part of particle index of refraction
m = particle mass loading in plume, g/cm^3
n = real part of particle index of refraction
N = particle number density, l/cm^3
P = pressure, atm
r = particle radius, μm
R = plume radius, cm
T_g = gas temperature, K
T_m = particle melting temperature, K
T_p = particle temperature, K
X_i = gas mole fraction (component i)
δf_i = nondimensional uncertainty interval, df_i/f_i
ρ = particle density, g/cm^3

Introduction

THE effectiveness of tactical missiles is largely dependent on the magnitude of their exhaust plume signatures. Exhausts from solid-propellant rockets contain substantial amounts of particulate matter, which scatters photons and thereby influences the radiation transport processes in the plumes and the radiative emission from the plumes.[1,2] Radiation scattering influences the plume flowfield properties and shock wave structure[3] and the aspect angle dependence of the signature, especially at near nose-on aspect angles.[4] Because of base heating, radiation emitted from rocket plumes also plays an important role in missile design.[5,6]

Plumes of aluminumized, composite solid-propellant rocket motors contain liquid and solid aluminum oxide particles. The size, density, temperature, phase, and velocity of these particles influence motor performance, nozzle design, base heat transfer, plume infrared signature, and environmental fallout. Most of the effort to characterize aluminum oxide particles has involved measuring their size distribution.[7-9] Konopka et al.[10] measured the imaginary part of the refractive index of aluminum oxide particles in the temperature range of 1700-3000 K for particles captured from the exhausts of two full-scale aluminized rocket motors. The measured values for the captured particles differed widely from those of commercial grade pure Al_2O_3 particles. Differences as large as a factor of 10 were found between the particles from the two rockets and differences of factors of 10-100 between the commercial grade Al_2O_3 particles and the rocket particles. Thus, there is considerable uncertainty in the value of the Al_2O_3 refractive index. Refractive index and particle size are very important properties for calculation of Mie scattering. Errors in size distribution and refractive index lead to errors in radiative scattering that, in turn, lead to errors in predicting radiative heating and signature magnitude.

In this study, a method is developed that systematically accounts for and evaluates the uncertainties involved in predicting infrared radiation emitted from aluminized rocket plumes. The approach consists of identifying the important parameters for plume infrared radiation calculations and then perturbing these parameters individually about a set of nominal values to establish their influence on the emitted radiation. Finally, all of the individual uncertainties are combined using an appropriate statistical method to obtain the uncertainty factor for the infrared plume signature. This analysis represents the first comprehensive effort directed at quantifying the level of uncertainty associated with rocket plume radiation signatures. It is conducted for a typical solid-propellant tactical rocket motor plume. The uncertainties are analyzed for the plume as viewed at aspect angles of 0 and 90 deg or nose-on and broadside, respectively.

Approach

Formulation

The theoretical analysis is based on the functional relationship for the radiation emitted from a rocket exhaust plume,

$$I = I(n,k,N,r,T_p,T_m,X_i,T_g,R,P) \quad (1)$$

The uncertainty in the value of I can be related to the uncertainty in the value of each of the parameters in Eq. (1).

Received Nov. 14, 1986; revision received March 9, 1987.

*Professor of Aerospace Engineering, Thermal Radiative Transfer Group, Department of Mechanical and Aerospace Engineering. Associate Fellow AIAA.

Error Analysis

Statistical error analysis can be applied to Eq. (1) if 1) the parameters are independent, 2) the uncertainties in the parameters are Gaussian distributed, and 3) the partial derivatives of the dependent variables with respect to the parameters are linear over the uncertainty interval.[11-13] When these conditions are satisfied, the total uncertainty is obtained by taking the square root of the sum of the squares of the partial derivatives times the uncertainties of the independent parameters,

$$\delta I = \left[\sum_i \left(\frac{\partial I}{\partial f_i}\delta f_i\right)^2\right]^{1/2} \tag{2}$$

This is sometimes referred to as the root-sum-square (RSS) technique. Care must be taken when applying this technique because the requirements for its application are seldom met; however, RSS error estimates are known to yield acceptable predictions when the random error sources do not meet all, or even most, of the restrictions.[12,13]

The mathematical expression for the plume signature uncertainty becomes

$$\delta I = \left[\left(\frac{\partial I}{\partial n}\delta n\right)^2 + \left(\frac{\partial I}{\partial k}\delta k\right)^2 + \left(\frac{\partial I}{\partial N}\delta N\right)^2 + \left(\frac{\partial I}{\partial r}\delta r\right)^2 + \left(\frac{\partial I}{\partial T_p}\delta T_p\right)^2 + \left(\frac{\partial I}{\partial T_m}\delta T_m\right)^2 + \sum_j \left(\frac{\partial I}{\partial X_j}\delta X_j\right)^2 + \left(\frac{\partial I}{\partial T_g}\delta T_g\right)^2 + \left(\frac{\partial I}{\partial R}\delta R\right)^2 + \left(\frac{\partial I}{\partial P}\delta P\right)^2\right]^{1/2} \tag{3}$$

when the RSS method is applied to Eq. (1). The sum on j in Eq. (3) accounts for the uncertainties in the mole fraction of the j gases in the plume. If more than one particle size exists, the terms involving N, r, and T_p must be summed over the number of particle size groups.

Application of the RSS method requires that each parameter is independent of all others, a situation that is not true for all the parameters in afterburning exhaust plumes. Some of the strongly coupled parameters are: particle temperature and gas temperature; gaseous species and gas temperature; and plume size, temperature, and pressure. In the current analysis, one parameter is varied at a time, while all other parameters are held constant at their nominal values. Consequently, any change in the overall plume intensity can be attributed to the parameter that was changed. This yields a numerical approximation to the rate of change of the plume intensity with respect to the variable parameter. In a strict sense, this evaluation of the variation in plume intensity is slightly in error; but if the parameter changes are small and the intensity changes are small, this approach yields an acceptable first-order evaluation of the plume radiation sensitivity with respect to the parameter of interest.

Uncertainty Parameters

The plume radiation emission error that can be related to a specific parameter is determined from numerical solutions with the value of the parameter perturbed from its nominal value. The individual terms in Eq. (3) represent the performance errors for specific parameters. Each term is composed of two parts: a weighting function and an uncertainty interval. The value of the weighting function is determined by evaluating the change in the nominal solution when a specific parameter is changed from its nominal value.

Uncertainty Intervals

The uncertainty interval is defined by inspecting the scatter in experimental data and theoretical results reported in the literature. Some of the uncertainty interval values are subject to interpretation. The uncertainty on n for Al_2O_3 was assumed to be ± 0.30, while that of k was taken to be ± 0.50.[10,14,15] The uncertainty on the mass loading

$$m = 4\pi r^3 \rho N/3 \tag{4}$$

becomes a function of the uncertainty of particle radius, particle density, and particle number density as

$$\frac{\delta m}{m} = \left[\left(\frac{3\delta r}{r}\right)^2 + \left(\frac{\delta \rho}{\rho}\right)^2 + \left(\frac{\delta N}{N}\right)^2\right]^{1/2} \tag{5}$$

The uncertainty in particle density and number density can be large.[10,14,15] The density of liquid and solid particles can differ by up to 20%. It can also change due to the type of structure of the particle and due to impurities in the particle. The number density is hard to predict and subject to errors of $\pm 25\%$.[16] The uncertainty in mass loading is directly related to the uncertainty in number density, as shown in Eq. (5) for constant particle radius and density. Consequently, the value of N was changed to yield a change in mass loading. However, when r was changed (to determine the sensitivity to particle size), the value of N was also changed to keep the particle mass loading constant.

A single size was used for the nominal particle size distribution. It is well known that real exhaust plumes contain a distribution of particle sizes.[9] Sensitivity to changes in the complex index of refraction for a distribution of particle sizes may be slightly different than the sensitivity obtained from a single size. However, the use of a single particle size is justified because the exact particle size distribution for afterburning plumes is not well known.[9,10]

The uncertainty interval for particle radius was taken to be ± 0.50, based mainly on Refs. 9, 10, and 15. The uncertainty interval of gas temperature[15,17-19] was taken as ± 0.10 and that for particle temperature[20] as ± 0.20 (although in shock tube tests, gas temperature error[15] can be held to ± 0.05). The heat transfer between the particles and the gases is very hard to model and predict. The melt temperature uncertainty interval was assumed to be ± 0.05.[15] There is some question as to what happens to the imaginary part of the index of refraction of Al_2O_3 at the melt temperature as the particles change phase.[10,15] Also, the particles do not change phase instantaneously.[21] The melting and solidification process for Al_2O_3 particles in plumes is not well understood. The uncertainty interval for the gas mole fractions was taken as ± 0.20 from turbulent flame studies.[17-19] The uncertainty interval for plume pressure was taken as ± 0.20, even though Ref. 16 shows much larger pressure uncertainties. The plume radius uncertainty interval was assumed to be ± 0.10. The uncertainty in the broadside plume radiating area is directly related to the plume radius uncertainty.

Results and Discussion

The standard infrared radiation model (SIRRM) numerical code was used to predict the infrared radiation from the plume flowfields. The flowfields were generated using the Standard Plume Flowfield (SPF-I) numerical code. Both of those codes are current and involve the best available physics in their calculations. The particle property data used was the original SIRRM data with the unity albedos changed to 0.9998.

The SPF-I code predicts rocket exhaust plume flowfield structure at low (0–70 km) altitudes.[22-25] It partially accounts for two-phase plumes in that it calculates the mole fraction of particle molecules at each axial and radial flowfield point, which can be converted to a number density of particles of a specific size. Because of this limitation, heat and mass transfer between the particles and gases are not accounted for. The SPF-I code includes the effects of viscous/nonviscous interactions, turbulent mixing, exhaust shock wave

Table 1 Nominal conditions for tactical rocket plume

Nozzle Exit Composition			
Gas	Mole fraction	Temperature, K	Pressure, atm
H_2O	0.103	2070	1.069
CO_2	0.0124	2070	1.069
CO	0.169	2070	1.069
Particle	Number density, $1/cm^3$	Temperature, K	Radius, μm
Al_2O_3	1.173×10^6	2470	1.5

	Plume Radiation Aspect angle	
Band, μm	90 deg I, W/sr	0 deg I, W/sr
2-3	7988	159.6
3-4	2412	18.2
4-5	8083	122.9
2-5	18,464	300.7

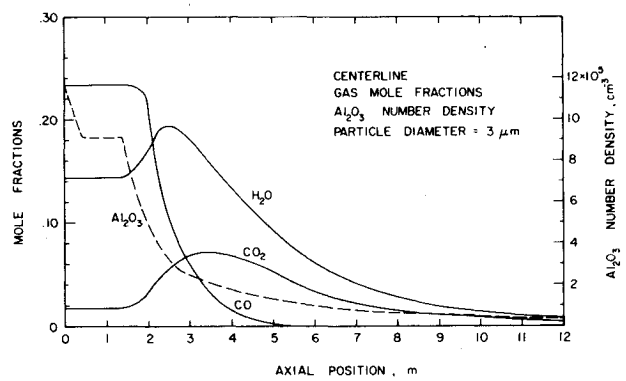

Fig. 1 Centerline gas mole fractions (left) and Al_2O_3 number density (right) as a function of an axial distance from the nozzle exit for the tactical rocket plume.

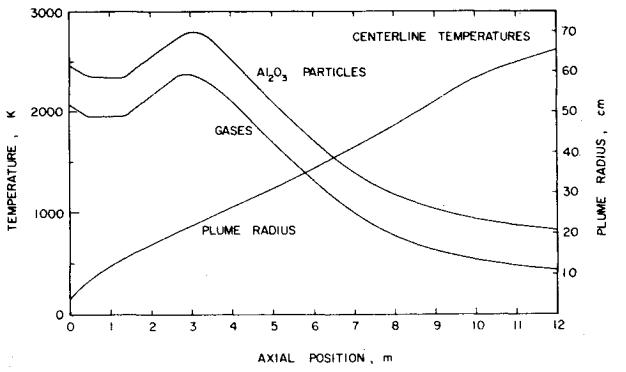

Fig. 2 Centerline gas and particle temperature (left) and plume radius (right) as a function of axial distance from the nozzle exit for the tactical rocket plume.

structure, including total pressure losses and the Mach disk, nonequilibrium chemistry, and gas/particle fluid dynamic interactions.

The SIRRM code calculates the infrared radiation emitted from exhaust plumes.[14,26] It considers multiple scattering and emission/absorption processes in a rigorous, but computationably tractable approach as a function of radial and axial position in the plume. The code contains options for different degrees of sophistication in treating particulate scattering. The six-flux option was used in the present analysis. SIRRM also contains an up-to-date data base for aluminum oxide, carbon, magnesium oxide, and zirconium oxide particles, and 26 i.r. active gases in the 2-25 um spectral range.

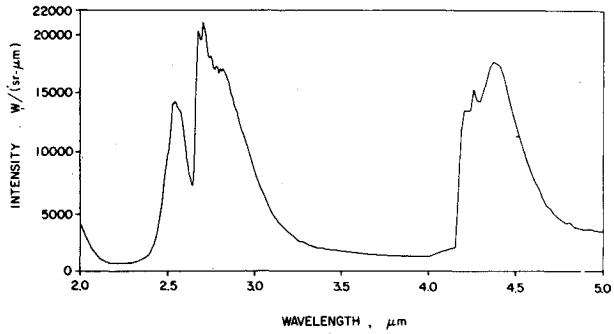

Fig. 3 Broadside spectral intensity of the tactical rocket plume as a function of wavelength.

The uncertainties were evaluated by running SIRRM code for the nominal plume, then individually perturbing each parameter of Eq. (3) above and below its nominal value, and rerunning SIRRM. The radiation results were plotted vs the perturbed parameter and the slope of the resulting curve was obtained at the nominal value of the parameter. This approach yielded the value of the weighting function of the emitted radiation with respect to each specific parameter.

Tactical Rocket Plume

The solid rocket motor propellant was assumed to be similar to the propellant used in the Space Shuttle solid rocket boosters (SRB-TP-H-1148). The combustion chamber pressure was 53 atm. The rocket nozzle had an expansion ratio (A/A^*) of 7.5, a 15 deg half-angle, and an exit diameter of 7.62 cm. The rocket was assumed to be flying at 4.6 km (15,000 ft) altitude at Mach 1. The exhaust plume contained 28.6% Al_2O_3 particles by weight. Table 1 gives the nominal nozzle exit composition and plume radiation for the tactical rocket motor.

Figures 1 and 2 give the rocket plume centerline values of the gas mole fractions, particle number density, and particle and gas temperatures as a function of axial distance behind the rocket nozzle exit. The plume radius is also shown as a function of distance behind the rocket. The plume undergoes afterburning, as indicated by the strong temperature rise 3 m downstream of the nozzle exit, the local maxima in the CO_2 and H_2O centerline mole fractions, and the rapid reduction of the CO mole fraction as a function of axial position.

The solid tactical rocket infrared signature was obtained for wavelength bands of 2-3, 3-4, 4-5, and 2-5 μm. The SIRRM code was run with a wavenumber step size of 10 1/cm at aspect angles of 90 and 0 deg (broadside and nose-on). It was run using the 6 flux option; the grid size was 18 axial positions, 10 layers, and 4 radial positions. The rocket was assumed to have a radius of 8 cm. The effect of the atmosphere between the plume and the detector was not considered.

Broadside

Figure 3 shows the broadside spectral intensity from the nominal tactical rocket plume. The projected side area is 19.42 m^2. The CO fundamental band at 4.6 μm, the H_2O 2.7 μm band, and the CO_2 2.7 and 4.3 μm bands are the most important radiation emission mechanisms. The Al_2O_3 particles emit a low-level continuum across the entire spectral interval. The magnitude of the intensity is large because it includes emission from the entire broadside area of the plume.

Figure 4 shows the nominal plume broadside station radiation for each of the four spectral bands as a function of axial

Table 2 Rocket uncertainty parameters at an aspect angle of 90 deg

Parameter f_i	δf_i	2-3 μm $\frac{\partial \bar{I}}{\partial f_i}$	2-3 μm $\left[\frac{\partial \bar{I}}{\partial f_i}\delta f_i\right]^2$	3-4 μm $\frac{\partial \bar{I}}{\partial f_i}$	3-4 μm $\left[\frac{\partial \bar{I}}{\partial f_i}\delta f_i\right]^2$	4-5 μm $\frac{\partial \bar{I}}{\partial f_i}$	4-5 μm $\left[\frac{\partial \bar{I}}{\partial f_i}\delta f_i\right]^2$	2-5 μm $\frac{\partial \bar{I}}{\partial f_i}$	2-5 μm $\left[\frac{\partial \bar{I}}{\partial f_i}\delta f_i\right]^2$
n	0.30	0.15	0.0020	1.77	0.2820	1.10	0.1089	0.75	0.0506
k	0.50	0.11	0.0030	0.43	0.0462	0.12	0.0036	0.14	0.0049
N	0.25	0.17	0.0018	0.29	0.0053	0.35	0.0077	0.27	0.0046
r	0.50	−0.12	0.0036	−0.12	0.0036	0.06	0.0009	−0.085	0.0018
T_p	0.20	2.65	0.2809	2.40	0.2304	1.08	0.0467	1.78	0.1267
T_m	0.05	−0.21	0.0001	−2.27	0.0129	−0.66	0.0011	−0.65	0.0011
X_{CO_2}	0.20	0.12	0.0006	0.012	0.0000	0.10	0.0004	0.10	0.0004
X_{H_2O}	0.20	0.55	0.0121	0.50	0.0100	0.022	0.0000	0.30	0.0036
X_{CO}	0.20	0	0.0000	0	0.0000	0.009	0.0000	0.004	0.0000
T_g	0.10	0.11	0.0001	0.80	0.0064	1.20	0.0144	0.66	0.0044
R	0.10	1.90	0.0361	1.80	0.0324	1.50	0.0225	1.65	0.0272
P	0.20	0.70	0.0196	0.50	0.0100	0.18	0.0013	0.40	0.0064
Sum	—		0.3594	—	0.6392	—	0.2075	—	0.2323
$\delta\bar{I}=(\text{sum})^{1/2}$	—		0.5999	—	0.7995	—	0.4555	—	0.4820

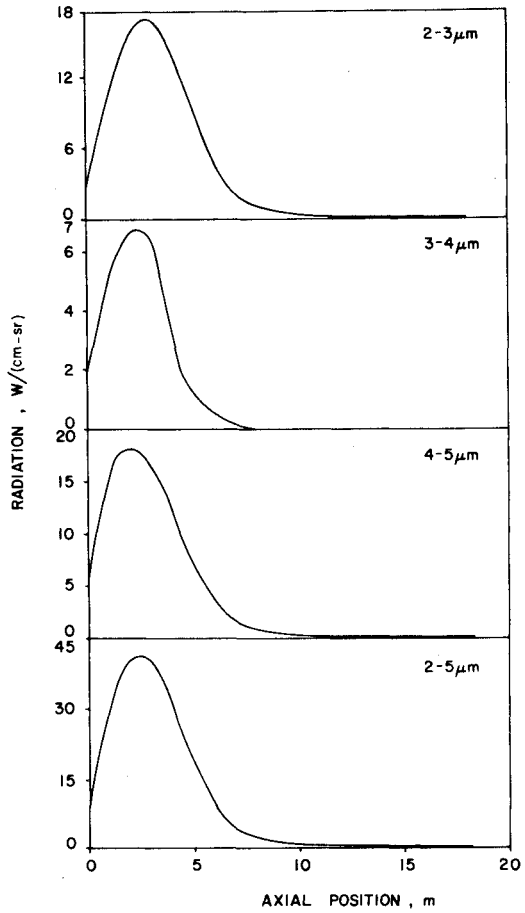

Fig. 4 Broadside station radiation of the tactical rocket plume as a function of axial position in the plume for four wavelength bands.

position behind the rocket nozzle exit. The most intense radiation is emitted in the afterburning region of the plume. The strongest emission comes from the 4-5 μm band, which is composed mainly of CO_2 and CO emissions. The 2 to 3 μm band produces significant broadside radiation, while the 3-4 μm band, which is mainly Al_2O_3 particle emission, is the weakest of the three bands shown. The overall broadside station radiation is shown in the lower graph for the entire 2-5 μm band. It is the sum of the three upper graphs. The emission from the tail part of the plume (10-18 m) is negligible.

Table 3 Ranking of uncertainty parameters for broadside view of solid rocket motor plume

	Spectral interval, μm							
	2-3		3-4		4-5		2-5	
Rank	f_i	%	f_i	%	f_i	%	f_i	%
1	T_p	78.1	n	44.1	n	52.5	T_p	54.5
2	R	10.0	T_p	36.1	T_p	22.5	n	21.8
3	P	5.5	k	7.2	R	10.8	R	11.7
4	X_{H_2O}	3.4	R	5.1	T_g	6.9	P	2.8
5	r	1.0	T_m	2.0	N	3.7	k	2.1
6	k	0.8	P	1.6	k	1.7	N	2.0

Table 2 summarizes the results of the uncertainty parameter analysis for the broadside plume signature of the tactical rocket. It contains the uncertainty parameters f_i, the certainty interval δf_i, and the uncertainty weighting function $\partial I/\partial f_i$. The uncertainty weighting function has a different value for each spectral band, because it represents the change in the band emission with respect to the change in a specific parameter. Table 2 also contains the value of the squared product of the uncertainty interval times the weighting function. This column is summed in the RSS method to obtain the plume signature uncertainty for each spectral band.

Table 2 gives the predicted nondimensional uncertainty in the plume signature in each of the four spectral bands considered. The uncertainty in plume signature is highest in the 3-4 μm band, where most of the radiation is due to aluminum oxide particles. The spectral region from 2-3 μm has the second highest infrared radiation signature uncertainty. The majority of the radiation in this spectral interval is due to CO and H_2O emissions. The spectral interval from 4-5 μm has the smallest radiation signature uncertainty. The CO_2 is a strong radiator in this spectral band (almost like a blackbody), so small changes in the uncertainty parameters do not influence the 4-5μm band emission very much.

The uncertainty of the plume infrared signature over the entire 2-5 μm wavelength band is predicted to be ±0.48 or the plume intensity is 18,464±8865 W/sr.

The information contained in Table 2 allows the uncertainty parameters to be rated in order of importance. The plume infrared signature is most sensitive to the uncertainty parameters with the largest value of $(\partial I/\partial f_i)\ \delta f_i$. Table 3 lists the six most important uncertainty parameters for each spec-

Table 4 Rocket uncertainty parameters at an aspect angle = 0 deg

Parameter f_i	δf_i	2-3 μm $\frac{\partial \bar{I}}{\partial f_i}$	2-3 μm $\left[\frac{\partial \bar{I}}{\partial f_i}\delta f_i\right]^2$	3-4 μm $\frac{\partial \bar{I}}{\partial f_i}$	3-4 μm $\left[\frac{\partial \bar{I}}{\partial f_i}\delta f_i\right]^2$	4-5 μm $\frac{\partial \bar{I}}{\partial f_i}$	4-5 μm $\left[\frac{\partial \bar{I}}{\partial f_i}\delta f_i\right]^2$	2-5 μm $\frac{\partial \bar{I}}{\partial f_i}$	2-5 μm $\left[\frac{\partial \bar{I}}{\partial f_i}\delta f_i\right]^2$
n	0.30	−2.20	0.4356	−2.55	0.5852	−2.05	0.3782	−2.30	0.4761
k	0.50	0	0.0000	0	0.0000	0	0.0000	0	0.0000
N	0.25	−1.28	0.1024	−1.60	0.1600	−0.60	0.0225	−1.00	0.0625
r	0.50	0.92	0.2116	0.49	0.0600	−0.27	0.0182	0.38	0.0361
T_p	0.20	2.00	0.1600	2.53	0.2560	0.95	0.0361	1.60	0.1024
T_m	0.05	0	0.0000	−0.65	0.0000	−0.12	0.0000	−0.08	0.0000
X_{CO_2}	0.20	0.03	0.0000	0	0.0000	0	0.0000	0.02	0.0000
X_{H_2O}	0.20	0.51	0.0104	0.80	0.0256	0.10	0.0004	0.30	0.0036
X_{CO}	0.20	0	0.0000	0	0.0000	0.08	0.0003	0.03	0.0000
T_g	0.10	1.75	0.0306	2.90	0.0841	2.90	0.0841	2.40	0.0576
R	0.10	2.80	0.0784	3.50	0.1225	3.20	0.1024	3.10	0.0961
P	0.20	0.43	0.0074	0.80	0.0256	0.10	0.0004	0.30	0.0036
Sum	—		1.0364	—	1.3190	—	0.6426	—	0.8380
$\delta\bar{I} = (\text{sum})^{1/2}$	—		1.0180	—	1.1485	—	0.8016	—	0.9154

tral interval in their order of importance and gives their percentage contribution to the total uncertainty. The plume broadside infrared radiation is most sensitive to the particle temperature and the real part of the particle refractive index. The plume radiation is also very sensitive to the plume radius. The imaginary part of the particle refractive index becomes very important in the 3-4 μm spectral interval, where most of the radiation is due to the particles. Other important parameters are the plume pressure and gas temperature.

Nose-on

Figure 5 shows the predicted nose-on spectral intensity as a function of wavelength for the nominal tactical rocket plume. The projected frontal area is 3.02 m^2. The signature has similar spectral characteristics to the broadside plume signature, except that the magnitude is much smaller. Recall that the rocket has a radius of 8 cm, so it blocks the radiation from the center of the plume. However, scattering in the plume allows some of the radiation from the center of the plume to eventually be directed in the nose-on direction.

Table 4 presents a tabulated summary of the RSS method applied to the nose-on plume signature. The same uncertainty parameters that were used for the broadside study are used here. Again, four spectral bands are considered. The uncertainty in the plume nose-on signature is greatest in the 3-4 μm band, where the Al_2O_3 particles are the most important radiators. Radiation scattered by the Al_2O_3 particles plays an important role in the nose-on signature because it allows radiation from the center of the plume to circumvent the blockage due to the rocket. The radiation emitted in the 4-5 μm band has the smallest uncertainty, but it still has over a 80% uncertainty. The uncertainty in the entire 2-5 μm wavelength band is predicted to be ±0.92 or the plume intensity is 300.7 ± 275.3 W/sr.

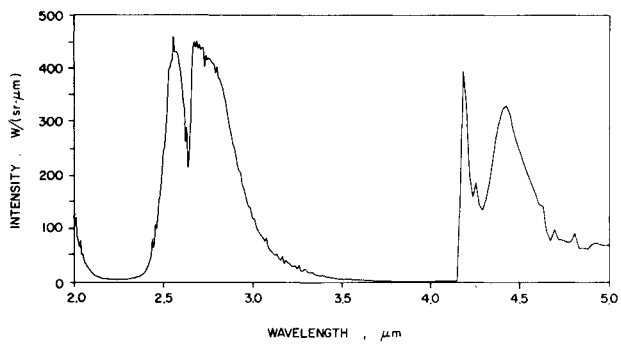

Fig. 5 Nose-on spectral intensity of the tactical rocket plume as a function of wavelength.

Table 5 lists the six most important uncertainty parameters and their percentage contribution to the total uncertainty for each spectral interval for the nose-on plume signature. The 2-3 μm spectral region is most sensitive to four uncertainty parameters related to the Al_2O_3 particles and the real part of the particle index of refraction, their size, temperature, and number density. Even though the particle emission is relatively small in this spectral interval, the radiation is very sensitive to the presence of the particles. In addition, the signature is quite sensitive to the uncertainty in the plume radius. For nose-on situations, one expects the plume signature to be sensitive to the plume radius because of partial blockage of the plume by the rocket.

In the 3-4 μm spectral interval, most of the radiation is emitted by the particles. Hence, the signature is most sensitive to the real part of the particle refractive index, particle temperature, and number density, as well as the plume radius. In addition, the plume signature is somewhat sensitive to the gas temperature and particle size. The imaginary part of the refractive index, which controls particle emission, does not contribute to the uncertainty because its weighting function is zero.

The plume signature in the 4-5 μm spectral interval is dominated by CO_2 and CO gas emissions; consequently, the plume radius and gas temperature are important uncertainty parameters. The real part of the particle refractive index is the most important uncertainty parameter, largely because it controls the radiation scattering. The four particle-related

Table 5 Ranking of uncertainty parameters for nose-on view of solid rocket motor plume

	Spectral interval, μm							
	2-3		3-4		4-5		2-5	
Rank	f_i	%	f_i	%	f_i	%	f_i	%
1	n	42.0	n	44.4	n	58.9	n	56.8
2	r	20.4	T_p	19.4	R	15.9	T_p	12.2
3	T_p	15.4	N	12.1	T_g	13.1	R	11.5
4	N	9.9	R	9.3	T_p	5.6	N	7.5
5	R	7.6	T_g	6.4	N	3.5	T_g	6.9
6	T_g	3.0	r	4.6	r	2.8	r	4.3

parameters (refractive index, temperature, number density, and size) are still relatively important.

The overall signature in the 2–5 μm spectral interval is most sensitive to the real part of the particle refractive index, particle temperature, and the plume radius. These parameters are followed by particle number density and gas temperature. It is interesting to note that the nose-on plume signature is not very sensitive to the imaginary part of the particle index of refraction. This occurs because the particle emission is very small relative to that of the gases. However, the real part of the particle index of refraction, which is closely related to scattering, is extremely important in signature evaluation.

In comparing the broadside and nose-on results, one should note that the nose-on plume signature is more uncertain than is the broadside signature. In general, the plume signature is most sensitive to the real part of the Al_2O_3 refractive index, particle temperature, and plume radius for both nose-on and broadside cases.

Conclusions

The objective of this study was to determine the influence of the uncertainty in each of the parameters that contributes to the uncertainty in the infrared radiation emission from rocket motor plumes, results were obtained for a tactical rocket plume for both broadside and nose-on aspect angles. The uncertainties for each parameter were combined by the root-sum-square method to yield overall plume emission uncertainties in four wavelength bands: 2–3, 3–4, 4–5, and 2–5 μm. The uncertainty in broadside emission from the tactical rocket plume was most sensitive to the uncertainty in the real part of the particle refractive index, particle temperature, plume radius, and particle melt temperature.

The uncertainty in the tactical rocket nose-on infrared plume signature was most sensitive to the uncertainty in the real part of the particle refractive index, particle radius, particle temperature, plume radius, particle mass loading, and gas temperature. In neither case was one uncertainty parameter most important for all the bands.

Based on the relative ranking of the uncertainty parameters investigated herein, it is recommended that future research activities be directed toward improving the predictability of the Al_2O_3 particle properties in the plume. The major cause of the uncertainty in the plume signature is strongly coupled to the uncertainties associated with the Al_2O_3 properties.

Acknowledgment

This research was sponsored by Sverdrup Technology, Inc., Arnold Air Force Station, Tennessee, with Dr. Robert A. Reed as technical monitor.

References

[1]Edwards, D.K. and Bobco, R.P., "Effect of Particle Size Distribution on the Radiosity of Solid Propellant Rocket Motor Plumes," *AIAA Progress in Astronautics and Aeronautics: Spacecraft Radiative Transfer and Temperature Control,* Vol. 83, edited by T.E. Horton, AIAA, New York, 1982, pp. 111–127.

[2]Pearce, B.E., "Radiative Heat Transfer within a Solid-Propellant Rocket Motor," *Journal of Spacecraft and Rockets,* Vol. 15, March–April 1978, pp. 125–128.

[3]Lyons, R.B., Wormhoudt, J., and Kolb, C.E., "Calculation of Visible Radiation from Missile Plumes," *AIAA Progress in Astronautics and Aeronautics: Spacecraft Radiative Transfer and Temperature Control,* Vol. 83, edited by T.E. Horton, AIAA, New York, 1982, pp. 128–148.

[4]Lyons, R.B., Wormhoudt, J., and Gruninger, J., "Scattering of Radiation by Particles in Low Altitude Plumes," *Journal of Spacecraft and Rockets,* Vol. 20, March–April 1983, pp. 189–192.

[5]Goulard, R. (ed.), "Molecular Radiation and Its Application to Diagnostic Techniques," NASA TM X-53711, Oct. 1967.

[6]Rochelle, W.C., "Review of Thermal Radiation from Liquid and Solid Propellant Rocket Exhausts," NASA TM X-53579, Feb. 1967.

[7]Strand, L.D., Bowyer, J.M., Varsi, G., Laue, E.G., and Gauldin, R., "Characteristics of Particulates in the Exhaust Plume of Large Solid-Propellant Rockets," *Journal of Spacecraft and Rockets,* Vol. 18, July–Aug. 1981, pp. 297–305.

[8]Hermsen, R.W., "Aluminum Oxide Particle Size for Solid Rocket Motor Performance Prediction," AIAA Paper 81-0035, Jan 1981.

[9]Girata, P.T. and McGregor, W.K., "Particle Sampling of Solid Rocket Motor (SRM) Exhausts in High Altitude Test Cells," *Progress in Astronautics and Aeronautics: Spacecraft Contamination: Sources and Prevention.* Vol. 91, edited by J.A. Roux and T.D. McCay, AIAA, New York, 1984, pp. 293–311.

[10]Konopka, W.L., Reed, R.A., and Calia, V.S., "Measurements of Infrared Optical Properties of Al_2O_3 Rocket Particles," *Progress in Astronautics and Aeronautics: Spacecraft Contamination: Sources and Prevention,* Vol. 91, edited by J.A. Roux and T.D. McCay, AIAA, New York, 1984, pp. 180–196.

[11]Beers, Y., *Introduction to the Theory of Error,* Addison-Wesley, Reading, MA, 1958.

[12]Zigrang, D.J., "Statistical Treatment of Data Uncertainties in Heat Transfer," AIAA Paper 75-0710, May 1975.

[13]Nelson, H.F., "Analysis of Jupiter Probe Heat Shield Recession Uncertainties," *AIAA Progress in Astronautics and Aeronautics: Outer Planet Entry Heating and Thermal Protection,* edited by Raymond VisKanta, Vol. 64, AIAA, New York, 1979, pp. 293–320.

[14]Ludwig, C.B., et al., "Standardized Infrared Radiation Model (SIRRM), Vol. 1: Development and Validation," AFRPL-TR-81-54, 1981.

[15]Konopka, W., Reed, R.A., Calia, V.S., and Oman, R.A., "Controlled Hot Gas/Particle Experiments for Validation of a Standardized Infrared Radiation Model," AFRPL-TR-81-44, July 1981.

[16]Wilson, K.H. and Thomas, P.D., "A Numerical Method for High-Altitude Missile Exhaust Plume Flowfields," *AIAA Progress in Astronautics and Aeronautics: Spacecraft Radiative Transfer and Temperature Control,* edited by T.E. Horton, Vol. 83, AIAA, New York, 1982, pp. 149–168.

[17]Chen, J.Y., Gouldin, F.C., and Lumley, J.L., "Second-Order Modeling of a Turbulent Non-Premixed H_2-Air Jet Flame with Intermittency and Conditional Averaging," *Heat Transfer in Fire and Combustion Systems,* edited by C.K. Law, Y. Jaluria, W.W. Yuen, and K. Miyasaka, HTD Vol. 45, ASME, New York, 1985, pp. 87–100.

[18]Chen, L.D. and Lew, A.K., "On Modeling Hydrocarbon Turbulent Diffusion Flames," *Heat Transfer in Fire and Combustion Systems,* edited by C.K. Law, Y. Jaluria, W.W. Yuen, and K. Miyasaka, HTD Vol. 45, ASME, New York, 1985, pp. 113–120.

[19]Faeth, G.M., Jeng, S.M., and Gore, J., "Radiation from Fires," *Heat Transfer in Fire and Combustion Systems,* edited by C.K. Law, Y. Jaluria, W.W. Yuen, and K. Miyasaka, HTD Vol. 45, ASME, New York, 1985, pp. 137–152.

[20]Mitchell, R.E., Tichenor, D.A., and Hencken, K.R., "Velocity in Burning Polydisperse Pulverized Coal Streams," *Heat Transfer in Fire and Combustion Systems,* edited by C.K. Law, Y. Jaluria, W.W. Yuen, and K. Miyasaka, HTD Vol. 45, ASME, New York, 1985, pp. 37–46.

[21]Henderson, C.B., "Effect of Crystallization Kinetics on Rocket Performance," *AIAA Journal,* Vol. 15, April 1977, pp. 600–602.

[22]Dash, S.M., Pergament, H.S., and Thorpe, R.D., "The JANNAF Standard Plume Flowfield Model: Modular Approach, Computational Features and Preliminary Results," *Joint Army-Navy-NASA-Air Force (JANNAF) 11th Plume Technology Heating Proceedings,* Chemical Propulsion Information Agency (CPIA), Pub. 306, July 1979, pp. 345–442.

[23]Dash, S.M. and Pergament, H.S., "The JANNAF Standard Plume Flowfield Model: Operational Features and Preliminary Assessment," *Joint Army-Navy-NASA-Air Force (JANNAF) 12th Plume Technology Meeting Proceedings,* Vol. II, Chemical Propulsion Information Agency, (CPIA) Publication 332, Dec. 1980, pp. 225–228.

[24]Dash, S.M., Pearce, B.E., Pergament, H.S., and Fishburne, E.S., "Prediction of Rocket Plume Flowfields for Infrared Signature Studies," *Journal of Spacecraft and Rockets,* Vol. 17, May–June 1980, pp. 190–199.

[25]Dash, S.M. and Thorpe, R.D., "Shock-Capturing Model for One-and-Two-Phase Supersonic Exhaust Flow," *AIAA Journal,* Vol. 19, July 1981, pp. 842–851.

[26]Ludwig, C.B., Malkmus, W., Walker, J., Slack, M., and Reed, R., "A Theoretical Model for Absorbing, Emitting and Scattering Plume Radiation," *AIAA Progress in Astronautics and Aeronautics: Spacecraft Radiative Transfer and Temperature Control,* Vol. 83, edited by T.E. Horton, AIAA, New York, 1982, pp. 111–127.